Optik 125 (2014) 7106–7112

Contents lists available at ScienceDirect

Optik

journal homepage: www.elsevier.de/ijleo

Remote sensing of surface reflective properties: Role of regularization and a priori knowledge

Shengcheng Cui[a,b,*], Shizhi Yang[a,b], Chengjie Zhu[a,b,c], Nu Wen[a,b,c]

[a] Key Laboratory of Optical Calibration and Characterization, Chinese Academy of Sciences, Hefei 230031, China
[b] Anhui Institute of Optics and Fine Mechanics, Chinese Academy of Sciences, Hefei 230031, China
[c] University of Chinese Academy of Sciences, Beijing 100049, China

ARTICLE INFO

Article history:
Received 3 December 2013
Accepted 10 July 2014

Keywords:
Inverse problems
Bidirectional reflectance distribution function (BRDF)
Albedo
Regularization
A priori information

ABSTRACT

Linear kernel-driven bidirectional reflectance distribution function (BRDF) models have been used for mapping albedo with single field-of-view satellite measurements such as Moderate Resolution Imaging Spectroradiometer (MODIS). Due to limited samplings and poor angular configurations available from these satellite remotely sensed data, BRDF models inversion is often plagued by numerical instability. In order to overcome the ill-posedness of the BRDF model inversion and robustly estimate terrestrial surface albedo, a regularization technique is employed for the cases where the number of observations is insufficient, or the angular distribution is poor. Emphasis is also placed on the combination of a priori knowledge with the regularized inversion. Numerical performances and case study results with ground measurements and MODIS observations suggest that the method is sound and robust for ill-posed BRDF inverse problems. The method presented in this study is promising for land surface reflective parameters retrieval even for regions where only sparse observations are available.

1. Introduction

Electromagnetic wave reflected from the Earth's surface at satellite sensors level records signals not only from the underlying surface but from the intervening atmosphere [1]. To better understand the interactions between the surface and the atmosphere, and its impacts on the climate due to land surface processes, it is of necessity to extract land surface reflective parameters from orbital observations. Methods for quantitative retrieval of information of interests from remote measurements in the reflected domain are a rapidly growing field and increasingly attract attention of remote sensing and climate communities. For instance, land surface BRDF can be estimated from satellite observations to capture the directional distribution of the reflected radiance field. Correspondingly, directional-hemispherical reflectance (which is also called black-sky albedo, BSA) and bi-hemispherical reflectance (which is also called white-sky albedo, WSA) can be obtained via performing integrals of BRDF in the viewing hemisphere and illumination hemisphere, respectively [2,3]. These two kinds of albedos are of great importance and constitute indispensable input quantities for climate models [4,5].

In quantitative remote sensing of terrestrial surface, the relationship between the state parameters x and collected observations y mixed with the noise component ε_y can be established by a forward model:

$$y = F(x) + \varepsilon_y \quad (1)$$

where F is referred to as analytic BRDF models for land surface parameters retrieval. Computing y given x is called forward problem while the mathematic process of inferring x from y is called inverse problem (Fig. 1).

However, in geophysics and remote sensing sciences, inversion problems are in nature ill-posed [6–10]. In fact, ill-posedness always arises out of the lack of information needed for solving inverse problems so that noises during the whole remote sensing processes (e.g., inherent instrument noise, misregistration, inconsistent atmospheric correction, etc.) will cause instability in the retrieval. To overcome this, a variety of studies that centered round exploitation of additional constraints were carried out over last decade. In order to obtain physically acceptable parameters, Li et al. [9] addressed the importance of implanting a priori knowledge into the BRDF model inversion. Practically, the a priori information can be constructed from the collected spaceborne or airborne remotely sensed data or in situ measurements. Incorporation of a priori

* Corresponding author at: Key Laboratory of Optical Calibration and Characterization, Chinese Academy of Sciences, Hefei 230031, China. Tel.: +86 551 65593056.
E-mail address: shchcui@126.com (S. Cui).

http://dx.doi.org/10.1016/j.ijleo.2014.08.089
0030-4026/

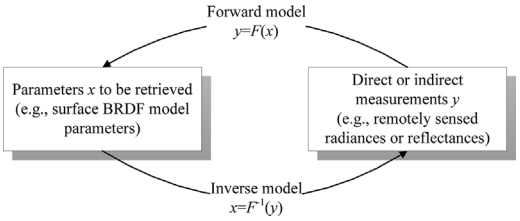

Fig. 1. Forward and inverse model in quantitative remote sensing of terrestrial surface.

information can increase numerical stability of the model inversion by making the original ill-posed inverse problem well-posed [9,11]. The multi-kernel least variance method (MKLV) developed by Gao et al. [12], selects least variance of albedo from various BRDF kernels as the best solutions and then combined these kernels as the most appropriate BRDF model. It is reported that the MKLV method is less sensitive to the sampling position and can operate well in small sample size. However, the MKLV method cannot deal with cases with less than three observations. Wang et al. [13,14] imposed a priori information from pure mathematical perspectives when performing regularized inversions. Quaife and Lewis [15] applied temporal smoothness constraints on BRDF model inversions using Lagrangian multipliers. Ways to obtain appropriate regularization parameters are not detailed in the literatures. However, crude selection of regularization parameters would limit the algorithm's efficiency and its applications. Cui et al. [16] improved the method for choosing regularization parameters and modified the algebra spectrum of the BRDF kernel matrix (i.e., replace tiny singular values with positive values after performing singular value decomposition (SVD) of the BRDF kernel matrix) to stable the BRDF model parameters estimates using the spectrum cut-off technique. Actually, the difference between these various approaches relies on how rigorously additional information is mathematically processed, and in particular, the uncertainties associated to this additional information.

In this study, we investigate the role of regularization in retrieving land surface reflective properties. In this paper, we first give a brief review of the selected BRDF model and a regularized inversion strategy established in our previous work. Then we extend the algorithm presented by integrating some additional constraints on the regularized BRDF inversion. Finally, selected case studies of BRDF model parameters inversion and albedo retrieval are presented to demonstrate the capability of our algorithm.

2. Algorithm description

2.1. Forward model

The forward model F in Eq. (1), needed for land surface BRDF and albedo retrieval, has mathematically the following form:

$$r_\lambda(\vartheta_s, \vartheta_v, \varphi) = f_{iso,\lambda}K_{iso} + f_{geo,\lambda}K_{geo}(\vartheta_s, \vartheta_v, \varphi) + f_{vol,\lambda}K_{vol}(\vartheta_s, \vartheta_v, \varphi) \tag{2}$$

where ϑ_s, ϑ_v and φ are solar zenith angle (SZA), view zenith angle (VZA) and the relative azimuth angle (RAA), respectively. This semiempirical kernel-driven model describes the BRDF of a pixel, r_λ, as a linear superposition of three types of kernels: (1) isotropic scattering kernel K_{iso}, which denotes the Lambertian scattering contribution and always equals to the constant of unity; (2) geometric-optical surface scattering kernel K_{geo}, which is derived by Wanner et al. [17] from surface scattering and geometric shadow casting theory [18]; and (3) volumetric scattering kernel K_{vol}, which is derived by Roujean et al. [19] from a single-scattering approximation of radiative transfer theory [20]. The combination of these kernels constitutes one of the most effective models for accurate reconstruction of BRDF, and has been proved to be suitable for most of the land cover types [2,3,21]. f_{iso}, f_{geo} and f_{vol} are Lambertian coefficient, roughness coefficient, and volume scattering coefficient respectively to be retrieved. In this study, the Ross–Li–Maignan (RLM) BRDF model [21] is used to model spectral surface bidirectional reflectance.

2.2. Ill-posedness of the inversion problem

With multiple cloudless measurements accumulated, Eq. (2) can be expressed in matrix notation:

$$\hat{\mathbf{r}}_{m\times 1} = \mathbf{K}_{m\times n}\mathbf{f}_{n\times 1} + \varepsilon_{\hat{\mathbf{r}}} \tag{3}$$

Here, $\hat{\mathbf{r}}$ is the reflectance vector, $\mathbf{f}$ is the BRDF parameters vector, $\mathbf{K}$ is the kernel matrix, m denotes the number of observations and n denotes the number of kernels. Given measurements at known angles, it is possible to invert Eq. (3) to obtain the kernel coefficients. For the overdetermined case (i.e., $m > n$), the least squares estimation may be employed to minimized the impact of observations errors. Then the aforementioned inverse problems can be solved by

$$\hat{\mathbf{f}} = arg\ \min\left\{\frac{1}{2}||\mathbf{K}\mathbf{f} - \hat{\mathbf{r}}||_D^2\right\} \tag{4}$$

where $||||_D^2$ denotes the 2-norm of a vector in the measurements space D.

However, sampling geometry is a major source of uncertainty in determining the BRDF shape. Noises due to insufficient samplings or poor angular configuration will make the condition of the kernel matrix $\mathbf{K}$ very large, and the so-called ill-posedness arises. This means that the least squares solution (LSS) (4) is nonunique and unstable. This can be made clear with the SVD of the kernel matrix $\mathbf{K}$:

$$\mathbf{K}_{m\times n} = \mathbf{U}_{m\times n}\Sigma_{n\times n}\mathbf{V}_{n\times n}^T \tag{5}$$

where matrices $\mathbf{U}$ and $\mathbf{V}$ are respectively with orthonormal columns $[\mathbf{u}_1, \ldots, \mathbf{u}_n]$ and $[\mathbf{v}_1, \ldots, \mathbf{v}_n]$, forming bases for the measurement space and the solution space, respectively. $\mathbf{\Sigma}$ is a diagonal matrix containing nonnegative singular values $(\sigma_1, \ldots, \sigma_n)$ in decreasing order. Because $\mathbf{\Sigma}$ is a diagonal matrix, the choice of these bases yields a one-to-one correspondence between components of the BRDF kernel coefficients and those of the measurements.

Substitution of Eq. (5) in Eq. (3) yields

$$\hat{\mathbf{r}} = \sum_{i=1}^{n}\sigma_i\left(\mathbf{v}_i^T\mathbf{f}\right)\mathbf{u}_i + \varepsilon_{\hat{\mathbf{r}}} \tag{6}$$

and the LSS can be written as

$$\hat{\mathbf{f}} = \sum_{i=1}^{n}\frac{\left(\mathbf{u}_i^T\hat{\mathbf{r}}\right)}{\sigma_i^2}\mathbf{v}_i \tag{7}$$

For indices i larger than a certain index p in Eq. (6), the σ_i are so small that all the terms $i > p$ do not have an effect on the measurement within the measurement error $\varepsilon_{\hat{\mathbf{r}}}$. This means that the measurement $\hat{\mathbf{r}}$ is insensitive to components $\mathbf{v}_i^T\mathbf{f}$ of the parameters $\mathbf{f}$ along base vectors $\mathbf{v}_i$ for $i > p$. So, in LSS of Eq. (7), only the first p terms play a role in the minimization of the residual norm. When the number of observations is insufficient or the angular distribution is poor, noise components in $\hat{\mathbf{r}}$ are divided by small singular values, their contribution to the retrieved BRDF parameters is amplified [16]. Hence, the task of the retrieval algorithm is to filter out the noise-dominated components of the solution and thus to retrieve only that part of the BRDF parameters about which information is present in the measurements. This part of the BRDF

parameters about which no information is present in the measurement defines the effective null-space of the problem. For this case, a suitable inversion algorithm is strongly desired and regularization is highly advantageous, the role of which played in the BRDF model estimates is to adjust the inversion procedure and to stable the solution.

2.3. Regularization

Since the solution to Eq. (3) is nonunique within the measurement error, additional condition constraints can be imposed to remove the ambiguity in the solution. Consider now a function that utilizes a least squares method with quadratic constraints in the form

$$\sum_i \varepsilon_i^2 + \gamma \sum_{j=1}^{n} (f_j - \bar{f})^2 \tag{8}$$

where γ is an arbitrary smoothing coefficient that determines how strongly the solution f_j is constrained to be near the mean $\bar{f}$. So, we may select a solution such that the measurement error is minimized while the solution is constrained to be close to the mean $\bar{f}$ such that

$$\frac{\partial}{\partial f_k}\left[\sum_i \left(\sum_{j=1}^{n} K_{ij} f_j - \hat{r}_i\right)^2 + \gamma \sum_{j=1}^{n} (f_j - \bar{f})^2\right] = 0. \tag{9}$$

This leads to

$$\sum_i \left(\sum_{j=1}^{n} K_{ij} f_j - \hat{r}_i\right) K_{ik} + \gamma (f_k - \bar{f}) = 0. \tag{10}$$

In matrix form, we have

$$\mathbf{K}^T\mathbf{K}\mathbf{f} - \mathbf{K}^T\hat{\mathbf{r}} + \gamma\mathbf{H}\mathbf{f} = 0 \tag{11}$$

From the point of functional analysis, the above doing is equivalent to adding a regularized penalty term $(\gamma/2)||\mathbf{H}^{1/2}\mathbf{f}||_X^2$ to the least squares estimation (4):

$$\hat{\mathbf{f}}(\gamma) = arg\ \min\left\{\frac{1}{2}||\mathbf{K}\mathbf{f} - \hat{\mathbf{r}}||_D^2 + \frac{\gamma}{2}||\mathbf{H}^{1/2}\mathbf{f}||_X^2\right\} \tag{12}$$

where X denotes the solution space, γ is also called regularization parameter (RP) in functional analysis and $\mathbf{H}$ represents the smoothness constraint matrix (SCM).

The regularization method is based on the Tikhonov regularization theory [22], the idea of which is to minimize the Tikhonov functional

$$J_\gamma(\mathbf{f}) = \frac{1}{2}||\mathbf{K}\mathbf{f} - \hat{\mathbf{r}}||_D^2 + \frac{\gamma}{2}||\mathbf{H}^{1/2}\mathbf{f}||_X^2, \tag{13}$$

i.e., to solve $\partial J_\gamma(\mathbf{f})/\partial\mathbf{f} = 0$ for the solution vector $\mathbf{f}$.

Making use of the SVD of $\mathbf{K}$, the regularized solution can be written as

$$\mathbf{f}_\gamma = \sum_{i=1}^{n} \frac{\sigma_i^2}{\sigma_i^2 + \gamma^2\delta_i^2} \frac{\left(\mathbf{u}_i^T\hat{\mathbf{r}}\right)}{\sigma_i}\mathbf{v}_i \tag{14}$$

Here, δ_i are the singular values of $\mathbf{H}$. Advantage of (14) over (7) is that the regularized solution makes use of a filter [16]

$$\chi_i = \frac{\sigma_i^2}{\sigma_i^2 + \gamma^2\delta_i^2} \tag{15}$$

which filters out the terms for which $\sigma_i \ll \gamma\delta_i$ and retains the terms for which $\sigma_i \gg \gamma\delta_i$. It is clear that a good choice of RP γ and SCM $\mathbf{H}$ is crucial for regularization.

2.4. Hybrid algorithm for regularization parameter γ

As seen from Section 2.3, γ plays a critical role in stabilizing the solution. It determines the strength of the regularization. If γ is too small, the solution is underconstrained and possibly unstable, while if γ is too large, the solution is overconstrained and large biases can be produced in the retrieval. The question arises as how to select an appropriate γ.

2.4.1. Determination of the initial γ

In Tikhonov regularization method, γ can be interpreted as the information index, which is defined as the ratio of variance of the measurement errors to that of the parameters to be retrieved [16]. Conceptually, it depends on the noise level and the information content in the measurements. Hence, we estimate the noise level of observations according to the SNR of optical sensors and calculate the regularization parameters by the expression $\gamma = \left[0.5\left(n_r^2 + \sigma_r^2\right)\right]^{1/2}$, where n_r denotes the noise-to-signal (NSR, i.e., the reciprocal of the SNR) of satellite sensors and σ_r is reflectance noise due to atmospheric correction [23]. For reference, Table 1 lists some specifications of the remote sensor MODIS.

2.4.2. Discrepancy principle

The discrepancy function is defined as

$$\Delta(\gamma) = ||Kf(\gamma) - \hat{r}||_D^2 - \varepsilon^2 \tag{16}$$

The damped Morozov's discrepancy principle (MDP) suggests choosing the regularization parameter γ in such a way that the error due to the regularization is equal to the error due to the measurements. That is to say, γ is chosen according to

$$||Kf(\gamma) - \hat{r}||_D^2 + \gamma^\beta||H^{1/2}f(\gamma)||_X^2 = \varepsilon^2 \tag{17}$$

where $\beta \in [1, +\infty)$, and the observation error ε is defined by $\varepsilon = ||r - \hat{r}||_D$.

The first derivative of the cost function $J(\gamma)$ is

$$J'(\gamma) = \frac{1}{2}||\mathbf{H}^{1/2}\mathbf{f}(\gamma)||_X^2, \quad \text{for all } \gamma > 0 \tag{18}$$

In terms of $J(\gamma)$ and $J'(\gamma)$, the damped discrepancy equation can be rewritten as

$$J(\gamma) + (\gamma^\beta - \gamma)J'(\gamma) = \frac{1}{2}\varepsilon^2 \tag{19}$$

For the sake of simplicity and easy coding, here only comes some conclusive equation. Detail derivations can be referred to Kunisch and Zou [24].

To get an optimum γ, the above hybrid algorithm is employed. First, the initial value of γ is determined using the signal-to-noise ratio (SNR) of optical sensors [16] and the reflectance noises [25]. Then, with this initial value, Newton's iterative method is employed to solve the discrepancy equation. Combing these two steps, a physical and optimal RP will be obtained. The presented algorithm adjusts the final regularization parameters adaptively according to the degrees of ill-posedness in the BRDF model inversion against measured reflectance. Fig. 2 illustrates the RP adjustment procedure corresponding to 16 test cases (S1–S16) with different number of samplings, which range from 8 to 1, containing the overdetermined ill-posed and the underdetermined ill-posed retrieval cases. Compared to the initial guesses, i.e., 0.006206 and 0.011175 for MODIS Bands 1 and 2 (see Table 1), respectively, the final RPs are all adjusted to a fixed level by solving the Morozov's discrepancy equation with Newton's iterative method.

Table 1
Technical specifications for MODIS reflective bands 1–7 and corresponding regularization parameters.

Band	Central wavelength (nm)	Bandwidth (nm)	Required SNR	Reflectance noise	RP
1	645	620–670	128	0.004	0.006206
2	858	841–876	201	0.015	0.011175
3	469	459–479	243	0.003	0.003601
4	555	545–565	228	0.004	0.004197
5	1240	1230–1250	74	0.013	0.013259
6	1640	1628–1652	275	0.010	0.007524
7	2130	2105–2155	110	0.006	0.007702

2.5. A priori selection of smoothness constraint matrix

The SCM is typically either the identity matrix, a diagonal matrix, or a discrete approximation of a derivative operator [8]. However, if **H** is badly conditioned, tiny singular values of the discrete kernel matrix cannot be completely filtered even with large regularization parameter γ, while the identity matrix can lead to over-constraint on the solution (12). Nonetheless, a matrix which is not positive definite will not impose adequate smoothness constraint on the severely ill-posed BRDF model kernels.

From Eq. (10), we can have

$$\mathbf{K}^T\mathbf{K}\mathbf{f} - \mathbf{K}^T\hat{\mathbf{r}} + \gamma(\mathbf{f} - \bar{\mathbf{f}}) = 0 \tag{20}$$

Note that the mean value of the BRDF parameters $\bar{f}_i = (1/N)\sum_{j=1}^{N} f_{i,j}$ with i = (iso, geo, vol) and N denotes the total number of land cover types which are fairly good representative of the Earth's land surfaces whose spectrum are accumulated and archived to build a priori knowledge database for land surface BRDF retrieval [9]. In comparison with Eq. (11), it is easy to get the SCM as

$$\mathbf{H} = \begin{bmatrix} 1-N^{-1} & -N^{-1} & -N^{-1} \\ -N^{-1} & 1-N^{-1} & -N^{-1} \\ -N^{-1} & -N^{-1} & 1-N^{-1} \end{bmatrix} \tag{21}$$

One can find that the SCM (21) has the same form as derived by Twomey [8]. This selection of the a priori SCM fairly provides suitable smoothness constraints for ill-posed inversions in which the amount of the smoothness constraints is controlled by the RP.

3. Case study results

In order to test the presented algorithm and to highlight the role of regularization for ill-posed BRDF inversions, both ground measurements and MODIS pixels are used.

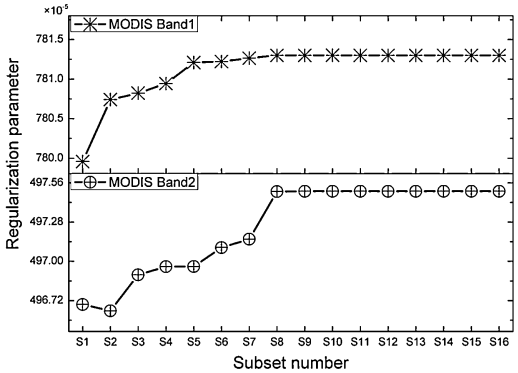

Fig. 2. Adjustment of regularization parameters for 16 cases with different number of observations (listed in Table 5).

3.1. Applied to overdetermined in situ measurements

Kimes [26] collected multi-angular BRDF data sets over orchard grass (hereafter referred to as *Kimes.orchgrass*). These data sets were collected in September near Beltsville in the red (580–680 nm) and the NIR (730–1100 nm) bands using a Mark III three-band radiometer with a 12° field of view. In this test, we use *Kimes.orchgrass* to check retrieval ability of our algorithm. There are 104 numbers of observations in *Kimes.orchgrass*. Angular sampling patterns and angular signatures of surface directional reflectance of *Kimes.orchgrass* are depicted in Fig. 3. Some other specific information of this dataset is given in Table 2.

It is obvious that hot spot effect is observed in *Kimes.orchgrass* data and there also exists large illumination condition as well as large viewing angles (see Fig. 3) in this data set. Inverting the linear BRDF model is typically ill-posed overdeterminated inverse problem so that no analytical solution could be obtained [7].

In Table 3, the root mean square error (RMSE) is calculated as

$$RMSE = \sqrt{\frac{1}{n_{bands}}\sum_{j=1}^{n_{bands}} e^2} \tag{22}$$

and the standard error of observations

$$e = \sqrt{\frac{1}{DoF}\sum_{i=1}^{n_{obs}} (\hat{r}_i - r_i)^2} \tag{23}$$

where *DoF* denotes the degree of freedom for the RLM BRDF model. n_{bands} represents the number of spectral bands, n_{obs} represents the number of observations, $\hat{r}$ and r denotes remote measured reflectance and predicted reflectance via the RLM BRDF model, respectively.

Then the joint red and near-infrared (NIR) band root mean square error is calculated by $RMSE_{\text{joint}}$:

$$RMSE_{joint} = \sqrt{\left(RMSE_{red}^2 + RMSE_{NIR}^2\right)/2} \tag{24}$$

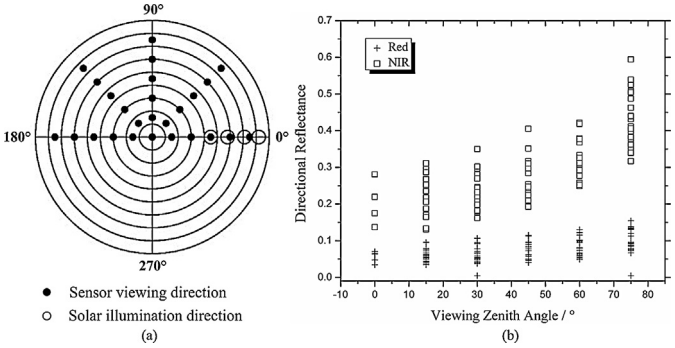

Fig. 3. (a) Angular samplings and (b) directional surface reflectance of *Kimes.orchgrass* (Kimes [26]). Radius of circles represents zenith angle at an interval of 10° (zero zenith angle is in the center) and polar angle represents azimuth (zero azimuth, East, is on the right). Solid circles refer to the viewing direction and open circles refer to the location of the sun.

Table 2
Specific information of *Kimes.orchgrass* data.

Land cover types	Number of SZA	SZA range (°)	Number of VZA	VZA range (°)	Vegetation coverage	LAI
Orchard grass	4	45–82	6	0–75	50%	1

Table 3
Comparisons results between different methods for *Kimes.orchgrass* in red band and NIR band.

Methods/models	Waveband	WSA	BSA			BRDF model parameters			$RMSE_{joint}$
			0°	30°	60°	f_{iso}	f_{vol}	f_{geo}	
Regularization	Red	0.0704	0.0641	0.0656	0.0727	0.0699	0.0314	0.0040	0.0483
	NIR	0.2851	0.2417	0.2526	0.3019	0.2541	0.2091	0.0062	
MKLV	Red	0.0686	0.0661	0.0667	0.0688	0.0680	0.0000	0.0007	0.0553
	NIR	0.2745	0.2656	0.2659	0.2735	0.3221	0.0038	0.0692	
RPV	Red	0.0707	0.0720	0.0713	0.0696	–	–	–	0.0493
	NIR	0.2739	0.2578	0.2624	0.2793	–	–	–	

Table 4
Bidirectional observations of a forest pixel over the southwestern United States during April, 2000 (DOY: day of year; RAZ: relative azimuth angle between the sensor and the sun).

DOY	VZA	RAZ	SZA	Band 1 (Red)	Band 2 (NIR)
97	51.6	243.9	28.4	0.047	0.166
98	38.5	−46.2	32.6	0.063	0.229
102	62.5	−39.5	34.6	0.065	0.226
103	7.1	−50.1	28.8	0.061	0.210
104	56.6	−246.5	25.6	0.045	0.166
105	29.6	−46.8	29.4	0.065	0.216
107	46.3	−43.1	30.3	0.058	0.222
108	28.5	−237	25.4	0.054	0.172
110	6.0	−228.6	25.7	0.063	0.199

Using the presented hybrid algorithm, the three BRDF model parameters are robustly retrieved and therefore the WSA as well as BSA is obtained physically. Since BSA is strongly SZA-depended, in Table 3, we also give estimations of BSA respectively at 0°, 30° and 60°. In comparisons with the MKLV method [12] and the nonlinear RPV BRDF model [27], the joint RMSEs against measurements are the lowest among other methods. In this context, the presented hybrid algorithm yields the best estimates of the RLM BRDF model parameters. Thus, the algorithm behaves well for the cases where there exist large illumination and viewing conditions.

3.2. Application to underdetermined MODIS data

To demonstrate the role of regularization in the underdetermined BRDF parameters estimates, the MODIS multi-angular samplings of a forest pixel in the southwestern United States during the period of April 6–19, 2000, which had been extracted by Gao et al. [28], were used (see Table 4).

In Table 5, each row displays the inversion results with different samplings randomly selected from all of the nine observations by using the presented regularization algorithm. The sampling sizes of Subsets 1–6 ranges from 8 to 3. The mean average percentage error (MAPE) is computed by

$$MAPE = \frac{1}{N}\sum_{i=1}^{N}\frac{x_i - x_0}{x_0} \times 100\% \quad (25)$$

where x_0 denotes the reference value for variable x_i.

The inversion results show that the retrieval of white-sky albedo and that of the isotropic kernel weights are very stable. However, geometric and volumetric kernel weights are variable especially in the visible red spectrum domain. It is because these two kernel functions are both dependent on the viewing geometries. This high variability can have several causes and underlying reasons. One is that the observation combinations from different angles can provide the inversion with different amount of information. Another is that the retrieved volumetric kernel and the geometric kernel are not orthogonal or even correlated and thus their relationship depends on the observation geometries.

Table 6 shows the surface albedo retrieved by the regularization algorithm with sparse angular samplings where the number of observations is less than 3. For one single observation, albedo retrieved with Subsets 8–16 are very close to the true value, except Subsets 12 and 16. The mean average percentage error is 7.97% in red band and 18.50% in near-infrared band. However, for the test cases with Subsets 9, 12 and 16, the retrieved white-sky albedo is obviously lower than the other values and the reference value. The same phenomenon can also be found in Table 2. The reflectance values of DOY108, DOY104 and DOY 97 are much lower than that of other DOYs. It perhaps caused by poor atmospheric correction due to inconsistent atmosphere conditions during the MODIS 16-day accumulation period. After removing these three subsets, the MAPE can achieve 0.25% for MODIS red band while 1.01% for MODIS NIR band. Although Subsets 9, 12 and 16 may have more noises than other subsets, the presented algorithm can still produce rational estimates according to the input reflectance.

Table 5
Inverted BRDF model parameters and white-sky albedos in red band and NIR band using sufficient observations ($n_{obs} \geq 3$).

Overdetermined cases	f_{iso_Red}	f_{geo_Red}	f_{vol_Red}	WSA_Red	f_{iso_NIR}	f_{geo_NIR}	f_{vol_NIR}	WSA_NIR
Reference value (N_{obs} = 9)	0.0688	0.0135	0.0590	0.0637	0.2216	0.0327	0.3525	0.2488
Subset 1 (N_{obs} = 8)	0.0664	0.0119	0.0725	0.0658	0.2207	0.0321	0.3569	0.2495
Subset 2 (N_{obs} = 7)	0.0654	0.0111	0.0739	0.0660	0.2253	0.0356	0.3503	0.2485
Subset 3 (N_{obs} = 6)	0.0641	0.0093	0.0725	0.0666	0.2268	0.0377	0.3518	0.2478
Subset 4 (N_{obs} = 5)	0.0658	0.0105	0.0811	0.0685	0.2272	0.0380	0.3536	0.2482
Subset 5 (N_{obs} = 4)	0.0648	0.0105	0.0932	0.0698	0.2293	0.0380	0.3275	0.2454
Subset 6 (N_{obs} = 3)	0.0640	0.0073	0.0745	0.0693	0.2290	0.0431	0.3643	0.2459
MAPE	−5.40%	−25.19%	32.12%	6.23%	2.16%	14.42%	−0.50%	−0.50%

Table 6
Inverted white-sky albedos in red band and NIR band using insufficient observations ($n_{obs} < 3$).

Underdetermined cases	WSA_Red	WSA_NIR
Subset 7 ($N_{obs} = 2$)	0.0658	0.2257
Subset 8 ($N_{obs} = 1$; DOY = 110)	0.0679	0.2144
Subset 9 ($N_{obs} = 1$; DOY = 108)	0.0541	0.1722
Subset 10 ($N_{obs} = 1$; DOY = 107)	0.0631	0.2414
Subset 11 ($N_{obs} = 1$; DOY = 105)	0.0646	0.2145
Subset 12 ($N_{obs} = 1$; DOY = 104)	0.0346	0.1278
Subset 13 ($N_{obs} = 1$; DOY = 103)	0.0633	0.2178
Subset 14 ($N_{obs} = 1$; DOY = 102)	0.0684	0.2379
Subset 15 ($N_{obs} = 1$; DOY = 98)	0.0665	0.2419
Subset 16 ($N_{obs} = 1$; DOY = 97)	0.0379	0.1340
MAPE	−7.97%	−18.50%

One can also see that when the number of observations is as small as three, the retrieval results obtained using the regularization algorithm are still stable as those obtained with more than seven observations. Moreover, the regularization algorithm is still workable even for the extreme case where there are less than three observations. In this context, our algorithm is adaptive. Especially, the results listed in Table 5 show that the improved algorithm can deal with cases without sufficient looks. Thanks to the reasonable regularization parameter and the smoothness constraint matrix, the ill-posed inverse problem can be solved effectively and meanwhile, the robust retrieval of the BRDF model parameters and surface albedo can be achieved.

From the trendlines of the WSA and the relative difference (Fig. 4), one can see that when the number of observations is not less than three, the results agree well with the reference value. But for cases with less than three observations, sampling itself will have an effect on the retrieval. The main cause is that the effective information from one single observation is very limited. So, additional constraints imposed on the BRDF model inversion by regularization is judged based on this single observation. Therefore, it is rational to foresee that if the input reflectance is of high quality, the presented regularization based hybrid inversion algorithm will always produce sound results with help of the a priori choice and the optimum determination of RP and SCM.

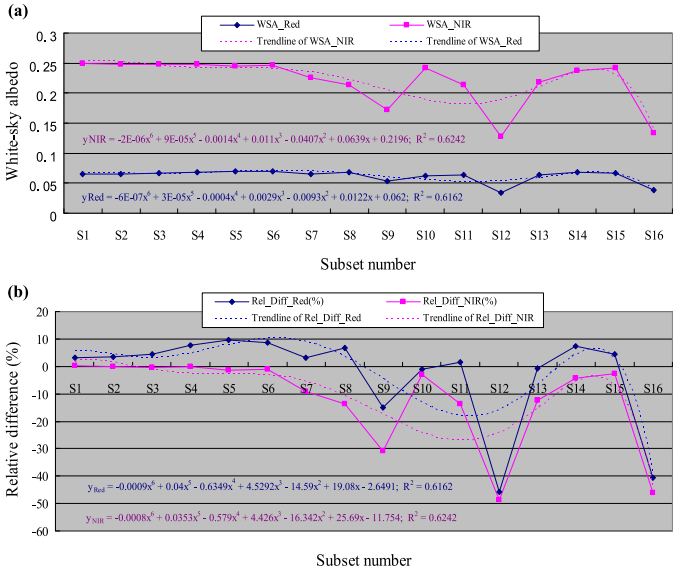

Fig. 4. (a) Retrieved results and their trendlines; (b) biases between the reference value and their trendlines in MODIS red and NIR bands.

4. Conclusions

We have proposed a regularization scheme for the land surface properties retrieval, which addresses the role of regularization and the use of a priori knowledge. Considering the ill-posed nature of remote sensing of land surface parameters, regularization techniques combined with a priori knowledge is by far one of the most effective tools to deal with problems faced in quantitative remote sensing, especially for the cases where there is insufficient information content in remotely sensed data. The presented algorithm is numerically stable, whatever the number of observations and the angular configuration. This good performance makes the presented algorithm a promising one. The regularization scheme is advantageous in less favorable conditions, i.e., the number of satellite looks is not enough to successfully invert land surface BRDF models using traditional approaches, or the information content in remotely sensed data is too limited to retrieve these variables with obvious physical meanings and physically acceptable magnitudes. In consequence, the risk of misuse and misinterpretation of remote sensing data can be largely reduced by using appropriate optimized regularization techniques. The regularization algorithm, serving as a reference one, will facilitate the application of high-spatial resolution satellite remote sensing imagery. As a final note, the proposed algorithm can also be of great value for the retrieval of multiple key parameters in the coupled land-surface system.

Acknowledgments

We are grateful to Dr. Feng Gao (USDA-ARS, USA) for allowing us to use their bidirectional measurements extracted from MODIS. Thanks would also given to Dr. Zhuosen Wang (University of Massachusetts, Boston, USA) for his helpful comments, and to MODIS land teams for all their previous works relating to this study. This work was supported by the National Natural Science Foundation of China (No. 41305019) and Anhui Provincial Natural Science Foundation (No. 1308085QD70).

References

[1] K.N. Liou, An Introduction to Atmospheric Radiative Transfer, second ed., Academic Press, San Diego, 2002.
[2] W. Lucht, C.B. Schaaf, A.H. Strahler, An algorithm for the retrieval of albedo from space using semi-empirical BRDF models, IEEE Trans. Geosci. Remote Sens. 38 (2000) 967–977.
[3] C.B. Schaaf, F. Gao, A.H. Strahler, et al., First operational BRDF, albedo and nadir reflectance products from MODIS, Remote Sens. Environ. 83 (2002) 135–148.
[4] S. Liang, Quantitative Remote Sensing of Land Surfaces, Wiley, New York, 2004, pp. 534 pp.
[5] J.V. Martonchik, C.J. Bruegge, A.H. Strahler, A review of reflectance nomenclature used in remote sensing, Remote Sens. Rev. 19 (2000) 9–20.
[6] D. Feng, A new formula for the linear constrained matrix inversion, in: Proceedings of IEEE Topical Symposium on Combined Optical, Microwave, Earth and Atmosphere Sensing, 22–25 March, 1993, pp. 60–63.
[7] M.M. Verstraete, B. Pinty, R.B. Myneni, Potential and limitations of information extraction on the terrestrial biosphere from satellite remote sensing, Remote Sens. Environ. 58 (1996) 201–214.
[8] S. Twomey, Introduction to the Mathematics of Inversion in Remote Sensing and Indirect Measurements, Dover, New York, 1996.
[9] X. Li, F. Gao, J. Wang, A.H. Strahler, A priori knowledge accumulation and its application to linear BRDF model inversion, J. Geophys. Res. 106 (D11) (2001) 11925–11935.
[10] A. Tarantola, Inverse Problem Theory and Methods for Model Parameter Estimation, SIAM, Philadelphia, 2005.
[11] I. Pokrovsky, O. Pokrovsky, J.L. Roujean, Development of an operational procedure to estimate surface albedo from the SEVIRI/MSG observing system by using POLDER BRDF measurements I. Data quality control and accumulation of information corresponding to the IGBP land cover classes, Remote Sens. Environ. 87 (2003) 198–214.
[12] F. Gao, C.B. Schaaf, A.H. Strahler, et al., Using a multi-kernel least variance approach to retrieve and evaluate albedo from limited bidirectional measurements, Remote Sens. Environ. 76 (2001) 57–66.
[13] Y. Wang, X. Li, Z. Nashed, et al., Regularized kernel-based BRDF model inversion method for ill-posed land surface parameter retrieval, Remote Sens. Environ. 111 (2007) 36–50.

[14] Y. Wang, C. Yang, X. Li, Regularizing kernel-based BRDF model inversion method for ill-posed land surface parameter retrieval using smoothness constraint, J. Geophys. Res. 113 (D13) (2008), D13101.1–D13101.11.
[15] T. Quaife, P. Lewis, Temporal constraints on linear BRDF model parameters, IEEE Trans. Geosci. Remote Sens. 48 (5) (2010) 2445–2450.
[16] S. Cui, S. Yang, Y. Qiao, Q. Zhao, et al., Adaptive regularized filtering for BRDF model inversion and land surface albedo retrieval based on spectrum cutoff technique, Optik 123 (2012) 250–256.
[17] W. Wanner, X. Li, A.H. Strahler, On the derivation of kernels for kernel-driven models of bidirectional reflectance, J. Geophys. Res. 100 (10) (1995) 21077–21089.
[18] X. Li, A.H. Strahler, Geometric-optical bidirectional reflectance modeling of the discrete crown vegetation canopy: effect of crown shape and mutual shadowing, IEEE Trans. Geosci. Remote Sens. 30 (1992) 276–292.
[19] J.L. Roujean, M. Leroy, P.Y. Deschamps, A bidirectional reflectance model of the earth's surface for the correction of the remote sensing data, J. Geophys. Res. 97 (18) (1992) 20455–20468.
[20] J.K. Ross, in: W. Junk (Ed.), The Radiation Regime and Architecture of Plant Stands, Artech House, Norwell, MA, 1981, p. 392.
[21] F. Maignan, F.M. Bréon, R. Lacaze, Bidirectional reflectance of Earth targets: evaluation of analytical models using a large set of spaceborne measurements with emphasis on the Hot Spot, Remote Sens. Environ. 90 (2004) 210–220.
[22] A.N. Tikhonov, V.Y. Arsenin, Solutions of Ill-posed Problems, John Wiley and Sons, New York, 1977.
[23] D.P. Roy, Y. Jin, P.E. Lewis, et al., Prototyping a global algorithm for systematic fire-affected area mapping using MODIS time series data, Remote Sens. Environ. 97 (2005) 137–162.
[24] K. Kunisch, J. Zou, Iterative choices of regularization parameters in linear inverse problem, Inverse Probl. 14 (1998) 1247–1264.
[25] D.P. Roy, J. Borak, S. Devadiga, et al., The MODIS land product quality assessment approach, Remote Sens. Environ. 83 (2002) 62–76.
[26] D.S. Kimes, Dynamics of directional reflectance factor distributions for vegetation canopies, Appl. Opt. 22 (9) (1985) 1364–1372.
[27] H. Rahman, B. Pinty, M.M. Verstraete, Coupled surface-atmosphere reflectance (CSAR) Model 2. Semiempirical surface model usable with NOAA advanced very high resolution radiometer data, J. Geophys. Res. 98 (11) (1993) 20791–20801.
[28] F. Gao, Y. Jin, X. Li, et al., Bidirectional NDVI and atmospherically resistant BRDF inversion for vegetation canopy, IEEE Trans. Geosci. Remote Sens. 40 (6) (2002) 1269–1278.